SSK-ICS LoRa: A LoRa-Based Modulation Scheme With Constant Envelope and Enhanced Data Rate

Aniket Mondal, Muhammad Hanif, *Senior Member, IEEE*, and Ha H. Nguyen, *Senior Member, IEEE*

***Abstract*— Long-range (LoRa) modulation is an orthogonal modulation scheme that uses linearly-modulated up chirps to represent information bits. Its constant envelope and good bit-error-rate performance make it one of the key players in establishing low-power wide-area networks for the Internet of things applications. However, LoRa modulation has low data rates. In this letter, we propose a new constant-envelope modulation scheme, named slope-shift-keying and interleaved-chirp spreading (SSK-ICS) LoRa modulation, that can deliver higher data rates than the conventional LoRa modulation scheme. Succinctly, the proposed SSK-ICS-LoRa modulation uses up chirps, down chirps, interleaved up chirps and interleaved down chirps to expand the signal set and hence can carry more bits per transmission symbol. For the same spreading factor and bandwidth consumption, the proposed scheme is able to improve the data rate of the conventional LoRa scheme up to 28.6%. We also present the optimal maximum-likelihood detectors for both coherent and non-coherent demodulators for the proposed scheme. Simulation results show that the proposed scheme outperforms LoRa modulation in both data rate and bit-error rate.**

***Index Terms*— Chirp-spread spectrum modulation, LoRa, LoRaWAN, ICS-LoRa, SSK-LoRa, FSCSS-IM.**

I. Introduction

AS THE Internet-of-things (IoT) paradigm is becoming more pervasive, many aspects of our lives are becoming easier, smarter, and more efficient. IoT enables automation of various tasks by using devices that sense the environment and communicate with other devices and/or humans to make intelligent decisions. In many cases, these devices are battery powered and communicate with other devices that are located at a large distance away. For such use cases, low-power wide-area networks (LPWANs) play an important role and have been deployed rapidly in recent years [1], [2].

One of the emerging LPWAN technologies is LoRaWAN [3]. This technology uses LoRa (long-range) modulation in its physical layer, which is basically a frequency-shift chirp spread spectrum modulation scheme [3]–[6]. In LoRa modulation, information bits are represented by linearly-modulated upchirps, where the instantaneous frequency of the transmitted chirp (symbol) spans the entire bandwidth. This makes LoRa modulation resilient to Doppler shifts and narrow-band interference. Also, an important and favorable property of chirps is their constant envelope, which allows low-cost and power-efficient non-linear amplifiers to be used for LoRa transmitters. These features, along with its good performance over long distances, make LoRa modulation an ideal candidate for IoT applications in which sensors are battery powered and communicate over long distances in the presence of interference [1]–[7].

LoRa modulation uses three different bandwidths (125 kHz, 250 kHz, and 500 kHz) and is characterized by a parameter called *spreading factor* (SF). These along with different code rates allow LoRa modulation to offer a wide range of achievable throughput, thus making it suitable for a multitude of applications, such as smart homes, smart cities, precision agriculture, environmental monitoring, etc., [2].

Although LoRa enjoys the afore-mentioned advantages, it has low data rates [8]–[11]. In particular, the highest data rate offered by LoRa modulation corresponding to the lowest SF value of 7 and the highest bandwidth of 500 kHz is about 27 kbps, which is quite limited for many applications. This is a reason that some LoRa modems also have frequency-shift-keying (FSK) transceivers so that the data rate can be increased to 50 kbps [7]. Adding a separate FSK transceiver helps to increase the data rates, but also requires more memory and computational resources, which, in turn, increases the manufacturing cost and power consumption of the devices.

With the objective of improving the data rates while maintaining the key benefits of LoRa modulation, researchers have proposed various modifications to the basic LoRa modulation [8]–[11]. Interleaved-chirp spreading LoRa-based (ICS-LoRa) modulation [9] is one of the LoRa-based modulation schemes that improves the data rates of LoRa modulation by using interleaved up chirps along with the up chirps used in the conventional LoRa modulation. Using interleaved chirps leads to one extra bit in every transmitted symbol. Furthermore, the envelope of the transmitted signals remains constant since interleaving of the frequency ramps does not alter the signal's envelope. On the other hand, in [8], the authors employ down chirps instead of interleaved up chirps to achieve higher data rates. Such a scheme, called slope-shift keying LoRa (SSK-LoRa), performs slightly better than both the conventional LoRa and ICS-LoRa schemes in terms of bit-error rate (BER). Furthermore, it also maintains the constant envelope of the transmitted signals while delivering the same data rate as that of ICS-LoRa.

In [10], the authors proposed phase-shift keying LoRa (PSK-LoRa) modulation, which increases the data rates of LoRa by embedding extra information bits in the initial phases of the chirps. Embedding extra information bits in the phase

Manuscript received December 6, 2021; revised January 7, 2022; accepted February 1, 2022. Date of publication February 9, 2022; date of current version May 10, 2022. This work was supported by the Internal Research Fund of Thompson Rivers University. The associate editor coordinating the review of this letter and approving it for publication was Z. Qin. *(Corresponding author: Muhammad Hanif.)*

Aniket Mondal and Muhammad Hanif are with the Department of Engineering, Thompson Rivers University, Kamloops, BC V2C 0C8, Canada (e-mail: mondala20@mytru.ca; mhanif@tru.ca).

Ha H. Nguyen is with the Department of Electrical and Computer Engineering, University of Saskatchewan, Saskatoon, SK S7N 5A9, Canada (e-mail: ha.nguyen@usask.ca).

Digital Object Identifier 10.1109/LCOMM.2022.3150666

requires the use of a coherent receiver, which can estimate the channel state information (CSI). In general, a coherent receiver is more complicated, and hence less desirable than a non-coherent receiver that can operate without the CSI.

More recently, the works in [11] and [13] proposed schemes that can significantly increase the data rates of LoRa modulation. Specifically, [11] applies the concept of index modulation [14] to represent a significantly large number of bits in one transmitted symbol, which is constructed as a unique combination of available up chirps. On the other hand, [13] uses two branches (in-phase and quadrature) of LoRa symbols to increase the data rate. It is pointed out that the scheme in [11] can work with a low-complexity non-coherent receiver, whereas the scheme in [13] requires a more complicated coherent receiver to work. One important point to note is that, although both schemes in [11] and [13] can improve the data rate very substantially and with only a slight degradation in BER performance, the transmitted signals in both schemes no longer have constant envelopes as in the conventional LoRa, ICS-LoRa and SSK-LoRa schemes [11]. As such, these schemes might not be suitable for devices that need to be equipped with low-cost non-linear amplifiers.

In this letter, we first present a new LoRa-based modulation scheme, named SSK-ICS LoRa. As the abbreviation suggests, this new modulation scheme is perceived by combining both ICS-LoRa and SSK-LoRa. Moreover, the letter also develops both optimal coherent and non-coherent detection algorithms for this new modulation scheme that are friendly to implement. Compared to ICS-LoRa and SSK-LoRa, the new scheme enjoys the same advantages of having constant envelope and can be demodulated without requiring the CSI (i.e., non-coherently), while delivering higher data rates. On the other hand, the key advantage of the proposed scheme over PSK-LoRa is that it can be demodulated non-coherently. In the following sections, we present the details of both the transmitter and receiver for the new SSK-ICS-LoRa scheme.

II. Proposed SSK-ICS-LoRa Modulation

Let SF be the spreading factor of the conventional LoRa modulation scheme. Then in the discrete-time complex baseband-equivalent representation, each chirp is defined by $M = 2^{\mathrm{SF}}$ samples. Denote the *basic* up chirp and *basic* down chirp by $x_0[n]$ and $y_0[n]$, respectively, where $n = 0, 1, \cdots, M-1$. They are mathematically given as,

$$x_0[n] = \frac{1}{\sqrt{M}} \exp\left\{ j \frac{\pi n^2}{M} \right\}, \tag{1}$$

and

$$y_0[n] = x_0^*[n] = \frac{1}{\sqrt{M}} \exp\left\{ -j \frac{\pi n^2}{M} \right\}. \tag{2}$$

In the conventional LoRa modulation, a total of M orthogonal up chirps are used to represent the information bits. The set of these M up chirps can be simply obtained from the basic up chirp as [8]

$$x_m[n] = x_0[\bmod (n+m, M)] = x_0[n+m], \tag{3}$$

and $m = 0, 1, \cdots, M-1$, and $\bmod(\cdot,\cdot)$ is the modulo operation. The last equality in the above expression holds because $x_0[n]$ is periodic with period M [8].

In SSK-LoRa modulation, a set of M orthogonal down chirps are used along with the M orthogonal up chirps. Thus, a total of $2M$ chirps are used. As such, $\mathrm{SF}+1$ bits are carried by every transmitted chirp. The M orthogonal down chirps used in SSK-LoRa modulation are given by [8]

$$y_m[n] = y_0[\bmod (n-m, M)] = y_0[n-m]. \tag{4}$$

In ICS-LoRa modulation, instead of the down chirps, interleaved up chirps are used. Specifically, an M-size interleaver, denoted by $\Pi(p[n])$ generates a set of M interleaved up chirps, thus, resulting in a total of $2M$ signals in the signal set. Here, the interleaver performs the following interleaving operation on the signal $p[n]$ with length M:

$$\Pi(p[n]) = \begin{cases} p[n], & 0 \le n < M/4 \\ p[n+M/4], & M/4 \le n < M/2 \\ p[n-M/4], & M/2 \le n < 3M/4 \\ p[n], & 3M/4 \le n < M. \end{cases} \tag{5}$$

In the proposed SSK-ICS-LoRa, the signal set consists of up chirps, down chirps, interleaved up chirps and interleaved down chirps. Thus, the signal set has the cardinality of $4M$. Thus, a total of $\log_2(4M) = \mathrm{SF} + 2$ bits can be sent in every symbol. Let $b_0, b_1, \cdots, b_{\mathrm{SF}+1}$ denote the information bits to be transmitted in each symbol. The mapping from information bits to symbols can be done as follows.[1] First, a decimal representation of the information bits, denoted by m, is computed

$$m = \sum_{i=0}^{\mathrm{SF}+1} b_i 2^i. \tag{6}$$

Then the transmitted signal (symbol) in the proposed SSK-ICS-LoRa, denoted by $s_m[n]$, is obtained by

$$s_m[n] = \begin{cases} x_{m'}[n], & 0 \le m < M \\ y_{m'}[n], & M \le m < 2M \\ x^{(\mathrm{I})}_{m'}[n], & 2M \le m < 3M \\ y^{(\mathrm{I})}_{m'}[n], & 3M \le m < 4M. \end{cases} \tag{7}$$

Here, $m' = \sum_{i=0}^{\mathrm{SF}-1} b_i 2^i$, whereas $x^{(\mathrm{I})}_{m'}[n] = \Pi\left(x_{m'}[n]\right)$ and $y^{(\mathrm{I})}_{m'}[n] = \Pi\left(y_{m'}[n]\right)$ are the interleaved up chirps and interleaved down chirps, respectively. Note that $|s_m[n]| = 1/\sqrt{M}$, which implies that SSK-ICS-LoRa modulation has a constant envelope property, similar to the conventional LoRa modulation.

Fig. 1 depicts the instantaneous frequencies of 16 symbols in the proposed SSK-ICS-LoRa modulation scheme. The first row shows 4 up chirps; the second 4 down chirps; the third 4 interleaved up chirps; and the fourth 4 interleaved down chirps. For comparison, among the displayed rows, LoRa modulation uses only the first row of symbols; SSK-LoRa the second row along with the first one; and ICS-LoRa the third row along with the first one.

Regarding spectral efficiency, each transmit symbol of the proposed SSK-ICS-LoRa modulation scheme carries a total of $\mathrm{SF}+2$ bits, whereas, that of the conventional LoRa modulation scheme carries SF bits. As such, the ratio of spectral efficien-

[1]Due to the orthogonality of the up chirps and down chirps, different mappings do not affect the BER.

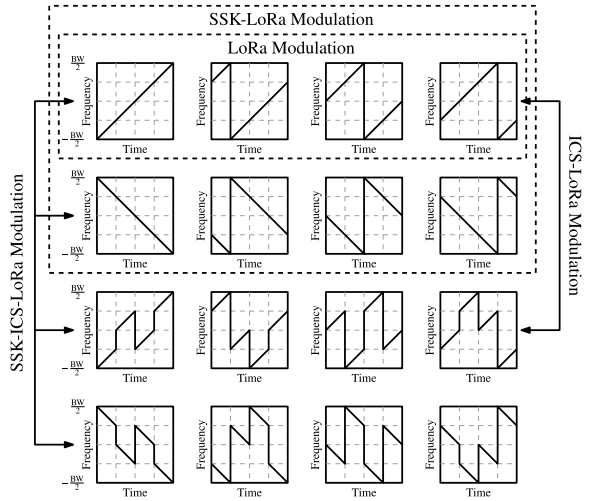

Fig. 1. Instantaneous frequencies of the transmitted symbols in LoRa, SSK-LoRa, ICS-LoRa, and SSK-ICS-LoRa modulation schemes.

cies between SSK-ICS-LoRa and LoRa modulation schemes is $(\mathrm{SF}+2)/\mathrm{SF}$. Since $7 \leq \mathrm{SF} \leq 12$, the data-rate improvement achieved by the proposed scheme is between $2/7 \approx 28.6\%$ and $2/12 \approx 16.7\%$.

III. Demodulation

In this section, we describe the optimal coherent and non-coherent maximum-likelihood (ML) detection of the proposed SSK-ICS-LoRa under additive white Gaussian noise (AWGN) and Rayleigh fading channels. To this end, we denote the synchronized baseband equivalent of the received signal by $r[n]$. Mathematically, $r[n]$ is given by

$$r[n] = hs_m[n] + w[n], \tag{8}$$

where h is the fading-channel gain, $s_m[n]$ is the transmitted signal, and $w[n]$ is a zero-mean white Gaussian noise. Without loss of generality, we presume that $E[|h|^2] = 1$, where $E[\cdot]$ denotes the expectation operation. As such, the noise variance is given by $E[|w[n]|^2] = 1/M\overline{\gamma}$, where $\overline{\gamma}$ is the average signal-to-noise ratio (SNR) of the received signal. Note that the instantaneous SNR is $\gamma = |h|^2\overline{\gamma}$. Also, for an AWGN channel, $h = 1$. Thus, $\gamma = |h|^2\overline{\gamma} = \overline{\gamma}$.

For completeness, we shall present both optimal coherent and non-coherent detection algorithms for the proposed scheme by following a similar approach in [8]. As mentioned before, since estimating the CSI increases the receiver's complexity, the non-coherent detection is more attractive for LoRaWAN devices.

A. Coherent Detection

The optimal coherent demodulator maximizes the likelihood function of the transmitted message. Since the noise is white and Gaussian, we can write the likelihood function as [8]

$$f(m|\mathbf{r},h) = \left(\frac{M\overline{\gamma}}{\pi}\right)^M \exp\left(-M\overline{\gamma}\sum_{n=0}^{M-1}|r[n]-hs_m[n]|^2\right). \tag{9}$$

Here, $\mathbf{r} = \big[r[0]\ r[1]\ \cdots\ r[M-1]\big]$. Noting that $|r[n] - hs_m[n]|^2 = |r[n]|^2 + |h|^2/M - 2\Re\{h^* r[n] s_m^*[n]\}$, (9) can be written as

$$f(m|\mathbf{r},h) = K\exp\left(2M\overline{\gamma}\Re\{h^*\sum_{n=0}^{M-1} r[n]s_m^*[n]\}\right), \tag{10}$$

where $\Re\{\cdot\}$ denotes the real component, and

$$K = \left(\frac{M\overline{\gamma}}{\pi}\right)^M \exp\left(-M\overline{\gamma}h^* - M\overline{\gamma}\sum_{n=0}^{M-1}|r[n]|^2\right). \tag{11}$$

Noting that K is independent of the message m, the ML detector can be expressed as

$$\widehat{m} = \underset{0<m<4M}{\operatorname{argmax}}\ \Re\left\{h^*\sum_{n=0}^{M-1} r[n]s_m^*[n]\right\}. \tag{12}$$

The ML detection rule described above requires performing correlation with a total of $4M$ signals, which can be computationally intensive, especially for large values of SF. In the following, we present a discrete-Fourier-transform (DFT) based detector which does not require correlation with such a large number of signals. To this end, we first note that [8]

$$x_m[n] = \sqrt{M}x_0[m]x_0[n]\exp\left(j\frac{2\pi mn}{M}\right), \tag{13}$$

$$y_m[n] = \sqrt{M}x_0^*[m]x_0^*[n]\exp\left(j\frac{2\pi mn}{M}\right), \tag{14}$$

and

$$\sum_{n=0}^{M-1} p[n]q[n] = \sum_{n=0}^{M-1}\Pi(p[n]q[n]) = \sum_{n=0}^{M-1}\Pi(p[n])\Pi(q[n]). \tag{15}$$

Here, (15) follows from the fact that interleaving operation does not alter the cumulative sum of a sequence, and it is distributive over the product of sequences.

Equation (7) implies that $s_m[n] = x_m[n]$ when $0 \leq m < M$. As such, for $0 \leq m < M$, we have

$$\begin{aligned}\sum_{n=0}^{M-1} r[n]s_m^*[n] &= \sum_{n=0}^{M-1} r[n]x_m^*[n] \\ &= \sqrt{M}x_0^*[m]\sum_{n=0}^{M-1} r[n]x_0^*[n]e^{-j\frac{2\pi mn}{M}} \\ &= \sqrt{M}x_0^*[m]R_1[m],\end{aligned} \tag{16}$$

where $R_1[m]$, $m = 0, 1, \cdots, M-1$, is the DFT of $r[n]x_0^*[n]$.

Similarly, for $M \leq m < 2M$, we have

$$\sum_{n=0}^{M-1} r[n]s_m^*[n] = \sqrt{M}x_0[m']R_2[m'], \tag{17}$$

where $m' = m - M$, and $R_2[m']$, $m' = 0, 1, \cdots, M-1$, is the DFT of $r[n]x_0[n]$.

Equation (5) implies that $\Pi\left(\Pi(p[n])\right) = p[n]$. Using this along with (15), we arrive at the following relationship for $2M \leq m < 3M$:

$$\begin{aligned}\sum_{n=0}^{M-1} r[n]s_m^*[n] &= \sum_{n=0}^{M-1} r[n]\Pi(x_{m'}^*[n]) \\ &= \sum_{n=0}^{M-1}\Pi(r[n])x_{m'}^*[n] = \sqrt{M}x_0^*[m']R_3[m'],\end{aligned} \tag{18}$$

where $m' = m - 2M$, and $R_3[m']$, $m' = 0, 1, \cdots, M-1$, is the DFT of $\Pi(r[n])x_0^*[n]$.

It can be similarly shown for $3M \leq m < 4M$ that

$$\sum_{n=0}^{M-1} r[n]s_m^*[n] = \sqrt{M}x_0[m']R_4[m'], \tag{19}$$

where $m' = m - 3M$, and $R_4[m']$, $m' = 0, 1, \cdots, M-1$, is the DFT of $\Pi(r[n])x_0[n]$.

Consequently, the ML detection rule given in (12) can be simplified to

$$\widehat{m} = \underset{0<m<4M}{\operatorname{argmax}} \Re\{h^* R_{\mathrm{c}}[m]\}, \tag{20}$$

where

$$R_{\mathrm{c}}[m] = \begin{cases} x_0^*[m]R_1[m], & 0 \leq m < M \\ x_0[m-M]R_2[m-M], & M \leq m < 2M \\ x_0^*[m-2M]R_3[m-2M], & 2M \leq m < 3M \\ x_0[m-3M]R_4[m-3M], & 3M \leq m < 4M. \end{cases} \tag{21}$$

B. Non-Coherent Detection

In the absence of CSI at the receiver, the optimal ML detection maximizes the likelihood function $f(m|\mathbf{r}) = E_H[f(m|\mathbf{r}, h)]$, where $f(m|\mathbf{r}, h)$ is defined in (9), and $E_H[\cdot]$ denotes expectation with respect to channel h. The probability density function of a Rayleigh fading channel gain is

$$f_H(h) = \frac{1}{\pi} \exp\left(-|h|^2\right). \tag{22}$$

Using (22) and performing some simplifications, we obtain

$$f(m|\mathbf{r}) = K' \exp\left(M\overline{\gamma} \left| \sum_{n=0}^{M-1} r[n]s_m^*[n] \right|^2\right), \tag{23}$$

where K' is independent of m. Thus, the optimal non-coherent ML detection rule for the proposed SSK-ICS-LoRa modulation is given by

$$\widehat{m} = \underset{0<m<4M}{\operatorname{argmax}} \left| \sum_{n=0}^{M-1} r[n]s_m^*[n] \right|^2. \tag{24}$$

Performing similar calculations done for the case of coherent detection, we can simplify (24) as

$$\widehat{m} = \underset{0<m<4M}{\operatorname{argmax}} |R_{\mathrm{nc}}[m]|^2, \tag{25}$$

where

$$R_{\mathrm{nc}}[m] = \begin{cases} R_1[m], & 0 \leq m < M \\ R_2[m-M], & M \leq m < 2M \\ R_3[m-2M], & 2M \leq m < 3M \\ R_4[m-3M], & 3M \leq m < 4M. \end{cases} \tag{26}$$

Finally, Fig. 2 depicts the receiver of the SSK-ICS-LoRa modulation scheme. Here, the original and interleaved received signals are multiplied by both basic up chirp and basic down chirp. Then, the DFT operations are carried out, which are then combined as in (21) or (26) for coherent or non-coherent detection, respectively. Afterwards, the information bits are obtained by performing decimal-to-binary conversion of the detected message through the argmax operation.

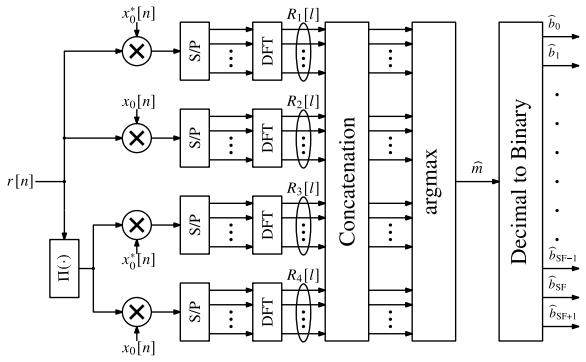

Fig. 2. Receiver for the SSK-ICS-LoRa modulation scheme.

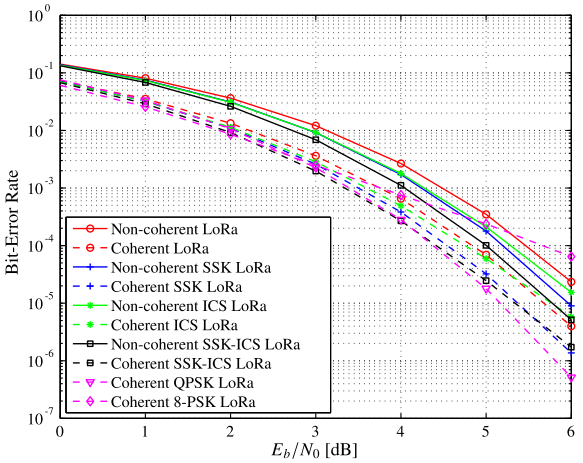

Fig. 3. Bit-error rate of coherent and non-coherent LoRa, SSK-LoRa, ICS-LoRa, SSK-ICS-LoRa, and PSK-LoRa modulation schemes for $\mathrm{SF} = 7$.

C. Computational Complexity Comparison

The demodulation of SSK-ICS-LoRa modulation symbols requires four DFT operations (one for each branch in Fig. 2), whereas the demodulators of SSK-LoRa and ICS-LoRa schemes use two DFT operations, and that of the conventional LoRa scheme uses only one DFT operation. As such, the number of operations in the demodulator of the proposed scheme is four times that of the conventional LoRa, and two times that of SSK-LoRa or ICS-LoRa schemes. As will be demonstrated by simulation results in the next section, such reasonable increase in computational complexity is well justified by the significant improvements in the data rate and slight improvements in the bit-error-rate performance of the proposed SSK-ICS-LoRa scheme.

IV. Simulation Results

In this section, we provide some simulation results comparing the error-rate performance of the proposed scheme with other LoRa-based modulation schemes in both AWGN and Rayleigh fading channels.

Fig. 3 plots BER curves versus E_b/N_0 for LoRa, SSK-LoRa, ICS-LoRa, SSK-ICS LoRa, and PSK-LoRa modulation schemes in AWGN channels. The BER values were obtained using a total of 10^9 symbols in Monte-Carlo simulations. Note that PSK-LoRa can only be demodulated coherently, whereas the BER curves for other schemes are shown for both coherent and non-coherent receivers. A few important observations can

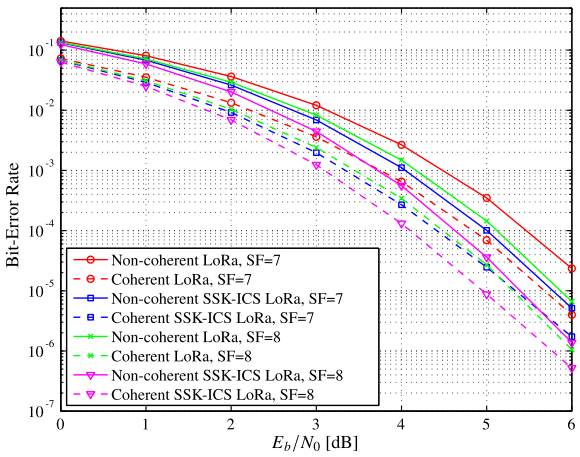

Fig. 4. Bit-error rate of coherent and non-coherent LoRa and SSK-ICS-LoRa modulation schemes for $\mathrm{SF} = 7, 8$.

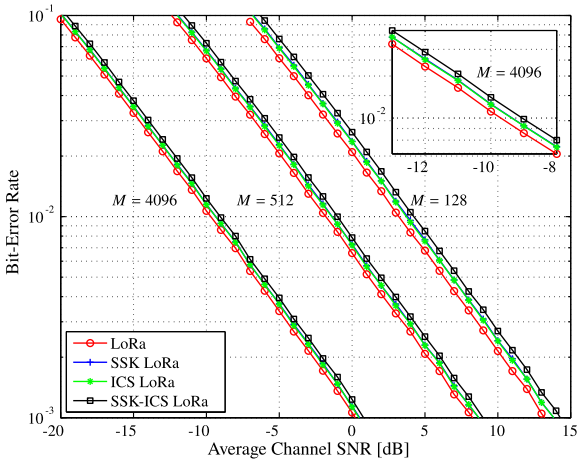

Fig. 5. Bit-error rate of non-coherent LoRa, SSK-LoRa, ICS-LoRa, and SSK-ICS-LoRa modulation schemes for $\mathrm{SF} = 7, 9, 12$ in a Rayleigh fading environment.

be made from Fig. 3. First, for any scheme (except PSK-LoRa), coherent detection always outperforms its non-coherent counterpart. Second, the proposed scheme performs slightly worse than QPSK-LoRa (both have the same data rate), but significantly better than 8-PSK-LoRa, LoRa, SSK-LoRa and ICS-LoRa. Specifically, the proposed scheme shows a gain of around 0.45 dB over the conventional LoRa scheme at the BER of 10^{-4} under both coherent and non-coherent detection. That is, the proposed SSK-ICS-LoRa performs better than the conventional LoRa in terms of both data rate and bit-error rate.

Fig. 4 compares the BER performance of LoRa and SSK-ICS LoRa for $\mathrm{SF} = 7, 8$. As expected, increasing SF improves the BER performance for both schemes.

Fig. 5 quantifies the receiver's sensitivity for LoRa, SSK-LoRa, ICS-LoRa, and SSK-ICS-LoRa schemes by plotting their BER performance curves against the average channel SNR, $\overline{\gamma}$, in a Rayleigh fading environment. Observe that all the schemes exhibit similar performance. However, the scheme that has a low data rate enjoys better receiver's sensitivity than the scheme that has a higher data rate. For example, LoRa modulation has the best sensitivity, but it has the lowest data rate. On the contrary, the proposed SSK-ICS-LoRa experiences a sensitivity loss of around 0.2 dB, but delivers the highest data rate. It is emphasized again that, when plotted against E_b/N_0 (SNR per information bit) as in Fig. 3 and Fig. 4, the proposed scheme actually has the best BER performance.

Finally, similar to LoRa modulation, the proposed scheme utilizes linearly-modulated chirps that span the whole bandwidth for data transmission, which makes it resilient to narrowband interference. However, the sensitivity loss incurred by the increased data rate of the proposed SSK-ICS-LoRa scheme results in a slightly more bit-error-rate degradation due to interference as compared to the conventional LoRa scheme.

V. Conclusion

In this letter, we have presented the new SSK-ICS-LoRa modulation scheme that employs down chirps along with interleaved up and down chirps to represent the information bits. The proposed scheme not only achieves higher data rates than the existing LoRa-based modulation schemes, but also enjoys better performance than its competitors for a wide range of signal-to-noise ratio per bit. An important property is that the proposed scheme has a constant envelope, which along with its superior performance and higher data rates than its competitors make it an ideal candidate for enabling low-power wide-area communications for IoT applications.

References

[1] U. Raza, P. Kulkarni, and M. Sooriyabandara, "Low power wide area networks: An overview," *IEEE Commun. Surveys Tuts.*, vol. 19, no. 2, pp. 855–873, 2nd Quart., 2017.

[2] J. P. S. Sundaram, W. Du, and Z. Zhao, "A survey on Lora networking: Research problems, current solutions, and open issues," *IEEE Commun. Surveys Tuts.*, vol. 22, no. 1, pp. 371–388, 1st Quart., 2020.

[3] (Nov. 2015). LoraAlliance. *LoRaWAN What is it? A Technical Overview of LoRa and LoRaWAN*. [Online]. Available: https://lora-alliance.org/wp-content/uploads/2020/11/what-is-lorawan.pdf

[4] L. Vangelista, "Frequency shift chirp modulation: The LoRa modulation," *IEEE Signal Process. Lett.*, vol. 24, no. 12, pp. 1818–1821, Dec. 2017.

[5] A. Augustin, J. Yi, T. Clausen, and W. Townsley, "A study of LoRa: Long range & low power networks for the Internet of Things," *Sensors*, vol. 16, no. 9, p. 1466, Sep. 2016.

[6] Q. Zhou, K. Zheng, L. Hou, J. Xing, and R. Xu, "Design and implementation of open LoRa for IoT," *IEEE Access*, vol. 7, pp. 100649–100657, 2019.

[7] *SX1261/SX1262 Development Kit User Guide*, SemTech, Camarillo, CA, USA, Mar. 2018.

[8] M. Hanif and H. H. Nguyen, "Slope-shift keying LoRa-based modulation," *IEEE Internet Things J.*, vol. 8, no. 1, pp. 211–221, Jan. 2021.

[9] T. Elshabrawy and J. Robert, "Interleaved chirp spreading LoRa-based modulation," *IEEE Internet Things J.*, vol. 6, no. 2, pp. 3855–3863, Apr. 2019.

[10] R. Bomfin, M. Chafii, and G. Fettweis, "A novel modulation for IoT: PSK-LoRa," in *Proc. IEEE 89th Veh. Technol. Conf. (VTC-Spring)*, Apr. 2019, pp. 1–5.

[11] M. Hanif and H. H. Nguyen, "Frequency-shift chirp spread spectrum communications with index modulation," *IEEE Internet Things J.*, vol. 8, no. 24, pp. 17611–17621, Dec. 2021.

[12] D. Zorbas and X. Fafoutis, "Time-slotted Lora networks: Design considerations, implementations, and perspectives," *IEEE Internet Things Mag.*, vol. 4, no. 1, pp. 84–89, Mar. 2021.

[13] I. B. F. de Almeida, M. Chafii, A. Nimr, and G. Fettweis, "Alternative chirp spread spectrum techniques for LPWANs," *IEEE Trans. Green Commun. Netw.*, vol. 5, no. 4, pp. 1846–1855, Dec. 2021.

[14] T. Mao, Q. Wang, Z. Wang, and S. Chen, "Novel index modulation techniques: A survey," *IEEE Commun. Surveys Tuts.*, vol. 21, no. 1, pp. 315–348, 1st Quart., 2019.